Conformational control of small GTPases by AMPylation

Katja Barthelmes[a,b,1], Evelyn Ramcke[a,1], Hyun-Seo Kang[a,b], Michael Sattler[a,b,2], and Aymelt Itzen[a,c,2]

[a]Center for Integrated Protein Science Munich, Department Chemistry, Technical University of Munich, 85747 Garching, Germany; [b]Institute of Structural Biology, Helmholtz Zentrum München, 85764 Neuherberg, Germany; and [c]Institute of Biochemistry and Signal Transduction, University Medical Center Hamburg-Eppendorf, 20246 Hamburg, Germany

Edited by Helen Mott, Department of Chemistry, University of Cambridge, Cambridge, United Kingdom, and accepted by Editorial Board Member Axel T. Brunger February 5, 2020 (received for review October 10, 2019)

Posttranslational modifications (PTMs) are important physiological means to regulate the activities and structures of central regulatory proteins in health and disease. Small GTPases have been recognized as important molecules that are targeted by PTMs during infections of mammalian cells by bacterial pathogens. The enzymes DrrA/SidM and AnkX from *Legionella pneumophila* AMPylate and phosphocholinate Rab1b during infection, respectively. Cdc42 is AMPylated by IbpA from *Histophilus somni* at tyrosine 32 or by VopS from *Vibrio parahaemolyticus* at threonine 35. These modifications take place in the important regulatory switch I or switch II regions of the GTPases. Since Rab1b and Cdc42 are central regulators of intracellular vesicular trafficking and of the actin cytoskeleton, their modifications by bacterial pathogens have a profound impact on the course of infection. Here, we addressed the biochemical and structural consequences of GTPase AMPylation and phosphocholination. By combining biochemical experiments and NMR analysis, we demonstrate that AMPylation can overrule the activity state of Rab1b that is commonly dictated by binding to guanosine diphosphate or guanosine triphosphate. Thus, PTMs may exert conformational control over small GTPases and may add another previously unrecognized layer of activity control to this important regulatory protein family.

posttranslational modifications | NMR | protein dynamics | small GTPases

Small GTPases (GTP hydrolases, also referred to as G proteins) are essential regulators of intracellular signaling and are involved in the control of diverse signal transduction pathways. Small GTPases act as molecular switches since they can exist in two fundamental activity states: They are inactive when bound to guanosine diphosphate (GDP) and active when bound to guanosine triphosphate (GTP). The transition between these states is regulated by dedicated enzymes such as guanine nucleotide exchange factors (GEFs) and GTPase activating proteins (GAPs) that stimulate activation or deactivation of small GTPases, respectively. GEFs activate G proteins by catalyzing the release of GDP and the rebinding of GTP that is in excess over GDP under physiological conditions (1). GAPs deactivate small GTPases by stimulating their intrinsic GTP-hydrolyzing activity and thereby return the G protein to the inactive GDP-bound state with the concomitant release of inorganic phosphate (P_i) (for a review on small GTPases, see ref. 2). In the active state, small GTPases propagate signaling via effector proteins that bind effectively to GTP- but not GDP-bound G proteins.

The central role of small GTPases in the coordination and regulation of intracellular signaling pathways requires a faithful and reliable communication of their activity state to upstream or downstream binding partners. To this purpose, small GTPases contain two highly important loop regions: switch I (i.e., α1–β2 loop) and switch II (i.e., β3–β4 loop) change their conformations according to the bound nucleotide. The switch regions are mainly conformational flexible and structurally disordered in the inactive GDP-bound state, but they become highly conformationally restrained and structurally ordered when being bound to GTP. Thus, binding partners of G proteins can discriminate activity states through differentially binding to the different structures of the switch regions in the GDP and GTP states.

Due to the exclusive significance of the switch loops for the binding of regulators and effectors, it is conceivable that these regions may also be subject to other layers of regulation such as posttranslational modifications (PTMs). A particularly intriguing example of manipulation of small GTPases is Rab1. This protein belongs to the Rab subfamily of small Ras-like GTPases and is involved in the regulation of vesicular trafficking between the endoplasmic reticulum and the Golgi apparatus. Furthermore, Rab1 plays a significant role in the formation of autophagosomes (3–5). Since Rab proteins are generally involved in regulating intracellular vesicular trafficking and therefore are frequently involved in the elimination of bacterial pathogens that have been taken up, it is not surprising that several bacteria have evolved with mechanisms to manipulate the activity of Rabs. For example, the causative agent of Legionnaires' disease *Legionella pneumophila* releases various bacterial proteins into the cytosol of the host cell that are dedicated to manipulate the activity of Rab1b during the infectious cycle directly. One of these is the bacterial protein DrrA (defect in Rab recruitment A, also referred

Significance

In order to respond to a diverse set of changing conditions, cells need to coordinate their intracellular protein networks spatially and temporally. In this respect, the family of small GTPases serves as molecular on/off switches that stimulate or inhibit discrete intracellular activities. Due to their central role in regulating cellular homeostasis, small GTPases are frequently targeted by bacterial pathogens, leading to manipulation of intracellular signaling. It is interesting to note that these pathogens covalently modify specific positions of small GTPases and thereby reprogram their activities to support infection. Using a combination of biochemistry and structural biology, we have discovered that these modifications can override the activity states of their targets in a manner not observed previously.

Author contributions: M.S. and A.I. designed research; K.B. and E.R. performed research; K.B., E.R., H.-S.K., M.S., and A.I. analyzed data; and M.S. and A.I. wrote the paper.

The authors declare no competing interest.

This article is a PNAS Direct Submission. H.M. is a guest editor invited by the Editorial Board.

Data deposition: Chemical shift assignments have been deposited in the Biological Magnetic Resonance Data Bank, http://www.bmrb.wisc.edu/ (accession nos. 50172–50183).

[1]K.B. and E.R. contributed equally to this work.

[2]To whom correspondence may be addressed. Email: sattler@helmholtz-muenchen.de or a.itzen@uke.de.

This article contains supporting information online at https://www.pnas.org/lookup/suppl/doi:10.1073/pnas.1917549117/-/DCSupplemental.

First published March 2, 2020.

to as SidM) that contains a central GEF domain (amino acids [aa] 340–533) that activates Rab1b and recruits it to the *Legionella* containing vacuole (LCV) (6–8). In addition, *Legionella* provides GAP activity through the secreted protein LepB and therefore is capable of deactivating Rab1b at later stages of infection (9). Furthermore, *Legionella* releases the Rab-effector protein LidA that can bind with high affinity to inactive and active Rab1b (7, 10). However, the activity of Rab1b is not only regulated at the level of protein–protein interactions, but also on the level of reversible PTMs (Fig. 1*A*). The N-terminal domain of DrrA (aa 1–339) is an AMP-transferase (ATase) and catalyzes the site-specific transfer of adenosine monophosphate (AMP) from adenosine triphosphate (ATP) to the switch II tyrosine 77 ($Tyr77_{Rab1b}$) of Rab1b in a process referred to as AMPylation or adenylylation (11). This modification can be hydrolytically reversed by the action of the *Legionella* enzyme SidD (12–14). Intriguingly, another PTM occurs at serine 76 of Rab1b: The *Legionella* protein AnkX is a phosphocholine transferase that attaches a phosphocholine moiety to $S76_{Rab1b}$ using cytidine diphosphate choline (CDP-choline) as a cosubstrate (15). This modification can be hydrolytically reversed by the *Legionella* enzyme Lem3 (16, 17).

Since the switch II region is important for the interaction with most upstream and downstream binding partners, AMPylation at $Tyr77_{Rab1b}$ and phosphocholination at $S76_{Rab1b}$ of Rab1b have been assumed to interfere sterically with binding of Rab1b interaction partners. Indeed, AMPylation and phosphocholination significantly impaired the deactivation of Rab1b:GTP by the *Legionella* GAP LepB or the mammalian GAP TBC1D20 (11, 16, 18). It was therefore concluded that these PTMs contribute to maintaining Rab1b in the active, GTP-bound state by interfering with GAP-stimulated GTP hydrolysis. The molecular mechanism for the interference with protein–protein interactions and the consequences of PTMs for the conformations of the switch regions, however, have not been investigated in the original publications. Our recent molecular dynamics simulation, however, indicated that AMPylation of Rab1b at Tyr77 may stabilize the conformation of both switch regions in an active form (19).

Interestingly, other small GTPases have also been observed to be modified with AMP in the course of infections. The mammalian Rho-family protein Cdc42 is targeted by the ATase IbpA of *Histophilus somni* or by VopS from *Vibrio parahaemolyticus* resulting in AMP modification in the switch I region at $Tyr32_{Cdc42}$ or $Thr35_{Cdc42}$, respectively (20, 21). These AMP modifications inhibited the interaction of active Cdc42 with mammalian downstream effectors and therefore inhibited signaling from that G protein (20–22). It is interesting to note that the AMP modifications are established on crucial amino acid side chains that are directly involved in binding the nucleotide: $Tyr32_{Cdc42}$ interacts with the γ-phosphate of GTP, and $Thr35_{Cdc42}$ coordinates the essential magnesium ion (23–25). Therefore, the presence of the AMP modification at these sites may affect nucleotide binding or the formation of the nucleotide-dependent inactive or active conformations.

Here, we systematically addressed the molecular consequences of AMPylation and phosphocholination of Cdc42 and Rab1b, using a combination of heteronuclear solution NMR experiments and biochemical characterization. We were surprised to observe that AMPylation, but not phosphocholination, overrides the nucleotide-dictated activity state of Rab1b by promoting the active conformation of the GTPase even in the GDP-bound form. In contrast to AMPylation of Rab1b within switch II, AMPylation of Cdc42 within switch I neither promotes the accumulation of the inactive nor the active conformation of the GTPase. Instead it results in intermediate states that presumably result from impaired nucleotide binding. Thus, PTMs such as AMPylation have the potential to contribute a second layer of regulation to small GTPases and may cause activity- and conformation-altering effects independent of the bound nucleotide.

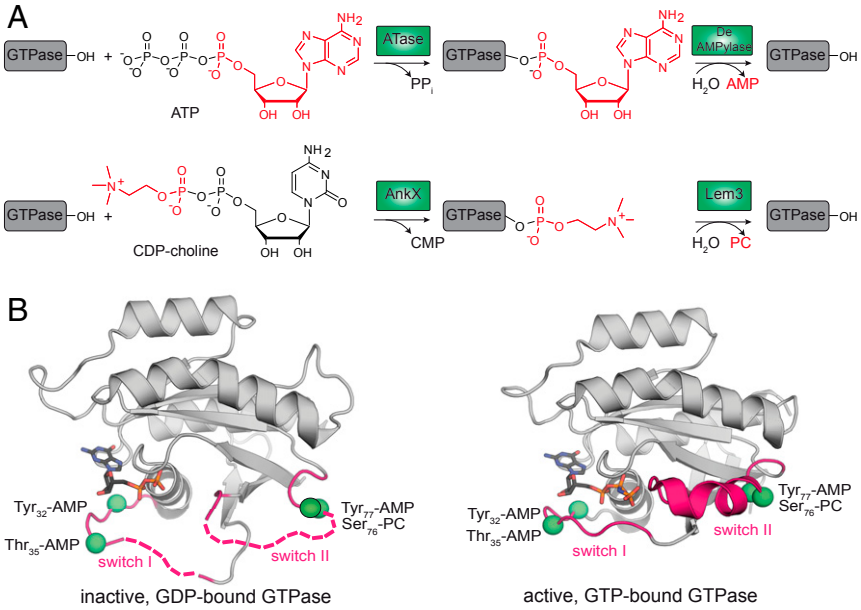

Fig. 1. PTMs of Rab1b and Cdc42 by bacterial pathogens. (*A*) AMP transferases (ATase) DrrA, VopS, and IbpA utilize ATP to transfer AMP covalently to Tyr77 of Rab1b, Thr35 of Cdc42, and Tyr32 of Cdc42, respectively. The deAMPylase SidD can hydrolytically cleave the AMP group from AMP_{Y77}–Rab1b. The phosphocholinase AnkX utilizes CDP–choline to transfer a phosphocholine group (PC) to Ser76 of Rab1b. The dephosphocholinase Lem3 hydrolytically cleaves the PC group. PP_i: pyrophosphate, CMP: cytidine monophosphate. (*B*) AMPylation (Rab1b or Cdc42) and phosphocholination (Rab1b) occur in the switch I and switch II regions of GTPases. In the inactive GDP state (*Left*), the switch regions are conformationally flexible, but they become highly structurally ordered in the active GTP state (*Right*). Green spheres: positions of amino acids with indicated PTMs, sticks: GDP (*Left*) and nonhydrolyzable GTP-analog GpNHp (*Right*). The position of posttranslationally modified amino acids in Rab1b and Cdc42 are indicated based on the Rab1-structures only, since these positions are homologous among the proteins (PDB code 3NKV, *Right*; 4LHV, *Left*) (11).

Results

AMPylation and phosphocholination are relatively new PTMs in the context of eukaryotic cells in general and in the area of small GTPases in particular (11, 20, 21) (Fig. 1*A*). Their molecular consequences on the structural and biochemical level are therefore only superficially understood. It is interesting to note that AMPylation and phosphocholination of small GTPases occur in the switch I and switch II regions that are important for communicating the activity state to physiological binding partners (Fig. 1*B*). We therefore experimentally addressed the biochemical and structural consequences of AMPylations occurring on Tyr77 of Rab1b (AMP_{Y77}–Rab1b), Tyr32 of Cdc42 (AMP_{Y32}–Cdc42), Thr35 of Cdc42 (AMP_{T35}–Cdc42), and phosphocholination on Ser76 of Rab1b (PC_{S76}–Rab1b).

AMPylation of Small GTPases Does Not Significantly Alter Nucleotide Binding. The switch regions intimately coordinate GDP and GTP. Consequently, any conformational alterations or covalent modifications in these sections may affect nucleotide binding. It has previously been demonstrated that AMPylation of Rab1b at Tyr77 does not alter the GDP/GTP binding to the switch regions and the rate of intrinsic GTP hydrolysis (12). The conservation of nucleotide binding properties in AMP_{Y77}–Rab1b and PC_{S76}–Rab1b was, however, expected since these switch II residues are not directly involved in GDP/GTP interactions. In contrast, the switch I modifications of Cdc42, AMP_{Y32}, and AMP_{T35} occur at the binding interfaces to the γ-phosphate or the essential magnesium ion, respectively (24, 25), potentially suggesting their roles in nucleotide binding and hydrolysis.

Therefore, we first tested whether the AMP modifications of Cdc42 at Tyr32 or Thr35 in the switch I region affect the rate of intrinsic nucleotide release (k_{off}). Since the nucleotide affinity is largely determined by the k_{off}, a change therein may be used as an indicator for the consequences of AMPylation on GDP and GTP affinities. To this purpose, unmodified and modified Cdc42 were preparatively loaded with the fluorescent *N*-methylanthraniloyl (mant) derivatives of GDP and GTP, i.e., mantGDP and mantGTP. The release of the labeled nucleotides was monitored in the presence of excess GDP or GTP by the decrease of mant-fluorescence and their rates determined by fitting to single exponentials (Fig. 2*A* and *SI Appendix*, Fig. S1). The rate of mantGDP release was ca. 30% decreased, whereas the rate of mantGTP release was increased by ca. 43% for both modification states relative to the unmodified Cdc42 protein. The faster rate of mantGTP release may be attributed to the known relevance of the Tyr32 and Thr35 moieties in binding the γ-phosphate and Mg^{2+}, respectively (23, 24). However, since the rates of nucleotide release are still slow on a physiologically relevant time scale (half-lives of 3,000 to 8,000 s), these alterations may be biologically insignificant.

Additionally, we determined the rate of intrinsic GTP hydrolysis. Unmodified and modified Cdc42 was loaded preparatively with GTP and the rate of GTP-to-GDP conversion was monitored by quantifying the GTP levels via nucleotide separation on reversed-phase chromatography (Fig. 2*B* and *SI Appendix*, Fig. S2). The rate of GTP hydrolysis was decreased by 40% for AMP_{T35}–Cdc42 ($2.0 \cdot 10^{-4}$ s^{-1}) and 75% for AMP_{Y32}–Cdc42 ($8.3 \cdot 10^{-5}$ s^{-1}) in comparison to the wild type ($3.3 \cdot 10^{-4}$ s^{-1}). Consequently, the AMP modifications of Cdc42 appear to stabilize and prolong the existence of the active state considerably. Nevertheless, since the slow rate of intrinsic GTP hydrolysis for the wild-type protein (half-life of 2,100 s) appears to be biologically negligible for returning the protein into the active state, the decrease of intrinsic Cdc42 deactivation is probably of low relevance.

In summary, the AMP modifications of Cdc42 in the switch region I alter its nucleotide-binding properties in a manner predictable from earlier structural and biochemical knowledge on the significance of Tyr32 and Thr35 for nucleotide interaction.

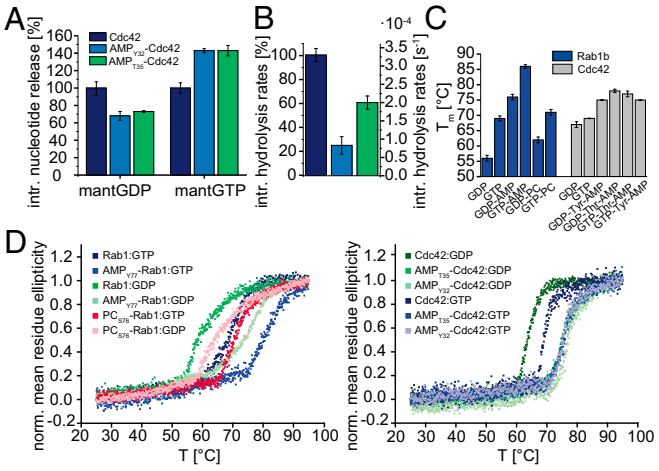

Fig. 2. AMPylation or phosphocholination stabilize small GTPases. (*A*) The rate of intrinsic nucleotide release of Cdc42 is affected moderately by AMPylation. The rates of intrinsic GDP and GTP release have been determined by monitoring the decrease in fluorescence of nucleotide mant-derivatives (progress curves are shown in *SI Appendix*, Fig. S1). (*B*) The rate of intrinsic GTP hydrolysis of Cdc42 is affected significantly by AMPylation. GTP-hydrolysis rates of indicated Cdc42 variants loaded preparatively with GTP have been determined from quantification of GTP contents using reversed-phase HPLC (progress curves are shown in *SI Appendix*, Fig. S2). (*C*) AMPylation or phosphocholination of Rab1b or AMPylation of Cdc42 stabilize the GTPases. The melting temperatures of indicated GTPase (GDP and GTP states, modified and nonmodified) have been determined from thermal unfolding by using circular dichroism signal changes as an indicator for thermal denaturation. (*D*) Circular dichroism signal changes in dependence of temperature (with respect to Fig. 2*C*) indicate thermal unfolding of modified and nonmodified Rab1b (*Left*) and Cdc42 (*Right*). The melting temperature is determined from the point of inflection of the data traces (the original spectra are shown in *SI Appendix*, Fig. S3).

However, the absolute changes in these properties are likely to be irrelevant for the biological functions of Cdc42.

Stability of Cdc42 and Rab1b in Response to PTMs. Because AMPylation of small GTPases does not change nucleotide-binding properties, we wondered whether PTMs could alter the protein stability of Rab1b and Cdc42. We therefore subjected wild-type and preparatively AMPylated Rab1b and Cdc42 and phosphocholinated Rab1b in both activity states to stability measurements and compared the unfolding behavior of these proteins. We have monitored thermal unfolding of Rab1b and Cdc42 in different GDP/GTP and modification states using the change in circular dichroism (CD) at $\lambda = 222$ nm and determined the melting points (T_m) at the point of inflection in the helical ellipticity (Fig. 2 *C* and *D* and *SI Appendix*, Fig. S3). Generally, GTPases were more stable in the GTP state as expected due to the ordered conformation of the switch regions and the interactions with the γ-phosphate. In addition, AMPylation of Rab1b and Cdc42 and phosphocholination of Rab1b significantly increased the stabilities of all proteins in both nucleotide-bound states. This effect was particularly pronounced for the AMPylation of Rab1b: AMPylation greatly stabilized the fold of Rab1b indicated by a shift in T_m by 20 °C ($T_{m,\ Rab1b:GDP}$ = 56 °C, $T_{m,\ AMP\text{-}Y77\text{-}Rab1b:GDP}$ = 76 °C).

In conclusion, Rab1b/Cdc42 AMPylation and Rab1b phosphocholination generally stabilize the GTPases. AMPylation at Tyr77 of Rab1b in particular appears to stabilize the fold and suggests that the AMP modification may have profound consequences on the GTPase structure.

Tyr77-AMPylation Forces Rab1b into the Active Conformation. The stabilization of Rab1b by PTMs (AMPylation and phosphocholination) in unfolding experiments suggests that the modifications

may alter the conformation of the GTPases directly. We therefore employed heteronuclear NMR methods to investigate conformational changes of modified proteins. To this purpose, we have produced ^{15}N-labeled Rab1b in the respective post-translationally modified states and in the active (GTP bound) or inactive (GDP bound) forms. These proteins were maintained in the GTP state by mutation of the conserved Q67 into alanine that inhibits the intrinsic GTPase activity (26). Maintaining the GTPases in the GTP state is crucial for the extensive duration in NMR experiments.

The structural changes of the active (GTP) and inactive (GDP) states of Rab1b were investigated by comparing ^{1}H,^{15}N heteronuclear single quantum coherence (HSQC) NMR spectra and analyzing in ^{1}H and ^{15}N chemical shift perturbations (CSP) (Fig. 3 *A* and *B*). CSPs plotted onto the crystal structure of AMP_{Y77}–Rab1b:GppNHp reveal differences in the conformations of the active and inactive state of Rab1b (Fig. 3*C*). In particular, residues in helix α1 close to the nucleotide binding site and the switch I and II regions are affected, potentially by the conformational rearrangement. Residues of switch II could not be assigned due to line broadening of the NMR signals indicating conformational dynamics on micro- to millisecond timescales. These residues are therefore missing in the CSP analysis. However, residues preceding switch II (I61–D63) show significant CSPs (>0.5 ppm) similar to residues in switch I. Additionally, helix α1 (which is located right above switch II) is influenced by the conformational switch from the active to inactive state (Fig. 3 *A* and *C*).

The effect of AMPylation on the activity state of Rab1b was investigated by an overlay of the respective ^{1}H,^{15}N-HSQC NMR spectra of AMP_{Y77}–Rab1b:GTP and AMP_{Y77}–Rab1b:GDP. The inactive AMPylated state AMP_{Y77}–Rab1b:GDP was obtained either by enzymatic hydrolysis of AMP_{Y77}–Rab1b:GTP by the GAP TBC1D20 or by direct AMPylation of Rab1b:GDP. Regardless of the preparation procedure, the chemical shifts of amides in AMP_{Y77}–Rab1b:GTP and AMP_{Y77}–Rab1b:GDP are in both cases identical (Fig. 3 *B* and *C*). Thus, AMPylation keeps Rab1b in the active state regardless of the type of nucleotide bound. In the case of Rab1b:GTP, AMPylation has no structural consequences and thus does not interfere with the active conformation (Fig. 3*D*). CSPs calculated for Rab1b:GTP vs. AMP_{Y77}–Rab1b:GTP and mapped onto the crystal structure of AMP_{Y77}–Rab1b:GppNHp (PDB code: 3KNV) reveal that only residues structurally adjacent to the AMP show small chemical shift changes with CSP values <0.2 ppm (Fig. 3*D*) (11). In comparison, CSPs calculated for Rab1b:GDP vs. AMP_{Y77}–Rab1b:GDP are large >0.7 ppm, affecting mainly the switch regions and helix α1, similar to the differences seen between the active and inactive states (*SI Appendix*, Fig. S4 *A* and *B*). These CSPs are very similar to those representing the conformational switch from the active to the inactive state or vice versa supporting the statement that AMP_{Y77}–Rab1b:GDP adopts the active conformation.

Further insight into the conformational switch between the active and inactive states of Rab1b was expected from an investigation of protein backbone motions, especially for the switch regions in the AMPylated states. An overlay of the ^{15}N–T_1, T_2 relaxation times and the {^{1}H}-^{15}N-heteronuclear NOE measured at 600 MHz reveals no significant difference in the global protein backbone motions (*SI Appendix*, Fig. S5). However, information on the dynamic behavior of the switch regions in the AMPylated-GTP- or GDP-bound state could not be obtained due to a lack of data points.

In order to confirm the observed conformational effects of the PTMs independently, we analyzed ^{31}P NMR signals of the bound nucleotides. The ^{31}P signals of GDP and GTP can be used as an indicator of conformational changes occurring in vicinity of the phosphates (in analogy to similar experiments conducted on the GTPase H-Ras; ref. 27). We compared one-dimensional ^{31}P NMR spectra of Rab1b:GDP, Rab1b:GTP, AMP_{Y77}–Rab1b:GDP, and AMP_{Y77}–Rab1b:GTP. Due to the expected strong chemical influence of the γ-phosphate group on the chemical shift of the β-phosphorus in the GTP-bound proteins, the β-phosphorus cannot be used as an indicator for conformational changes (*SI Appendix*, Fig. S6). However, the α-phosphorus is located farther from the γ-position and thus its chemical shift has been used for analysis. Notably, the α-^{31}P chemical shift is identical for active state conformation previously observed for Rab1b:GTP, AMP_{Y77}–Rab1b:GDP, and AMP_{Y77}–Rab1b:GTP, but different for the inactive Rab1b:GDP (*SI Appendix*, Fig. S6). Consequently, ^{31}P-NMR spectroscopy supports the previously observed activating effect of Tyr77 AMPylation in Rab1b. In summary, AMPylation of Tyr77 unexpectedly results in the conformational stabilization of the active Rab1b state regardless of binding to GTP or GDP.

Ser76-Phosphocholination of Rab1b Does Not Interfere with Conformational Switching. The structural impact of phosphocholination on Rab1b was investigated in analogy to the experiments for Rab1b AMPylation. First, we produced active PC_{S76}–Rab1b:GTP isotopically labeled with ^{15}N. We then recorded ^{1}H,^{15}N-HSQC experiments for PC_{S76}–Rab1b:GTP in defined GTP and GDP states to investigate conformational changes due to PC modifications. (Fig. 4*A* and *SI Appendix*, Fig. S7*A*). The conversion of different nucleotide and modification states are changed by using either the GAP TBC1D20 (GTP to GDP) or the dephosphocholinase Lem3, respectively.

Significant NMR spectral changes of unmodified Rab1b are observed between the GTP to the GDP states (*SI Appendix*, Fig. S7 *A* and *B*). The presence of the PC group in Rab1b does not influence the conformational transitions of the switches in the different nucleotide forms since the ^{1}H,^{15}N-HSQC spectra appear to be virtually identical (Fig. 4 *A* and *B*). When plotted onto the crystal structure of AMP_{Y77}–Rab1b:GppNHp (11), only small chemical shift perturbations are visible close to the PC modification site, which reflect the covalent attachment of the phosphocholine moiety. Consequently, the conformations of Rab1b are independent of the presence of PC at Ser76 and identical CSPs are observed in the transitions of Rab1b:GTP to Rab1b:GDP and PC_{S76}–Rab1b:GTP to PC_{S76}–Rab1b:GDP (*SI Appendix*, Fig. S7). Thus, phosphocholination of Rab1b at Ser76 does not affect the nucleotide-determined conformational distribution of Rab1.

AMPylation of Cdc42 Perturbs the Inactive and Active Conformations. In analogy to the experiments of AMPylated Rab1b, we characterized conformational effects of Cdc42-AMPylation at Tyr32 and Thr35. The hypothesis emerged from our biochemical experiments that the prolonged duration of the active state of AMP-modified Cdc42 might be caused by direct conformational rearrangements (Fig. 2*B*). In a first experiment, the expected transition from the active GTP-bound to the inactive GDP-bound state of unmodified Cdc42 could be observed on a ^{15}N-labeled protein sample through large shifts of the peak positions in the ^{1}H,^{15}N-HSQC-NMR spectra (*SI Appendix*, Fig. S8*A*). CSPs plotted onto the crystal structure of Cdc42:GDP (PDB code: 1NF3; ref. 28) revealed changes in the helix α1 close to the nucleotide binding site and for the residues of switch II (*SI Appendix*, Fig. S8*B*). Residues of switch I could not be assigned due to line broadening of the signals in the NMR spectra as result of the dynamic behavior of the switch regions and are therefore missing in the CSP analysis.

The presence of the AMP group in AMP_{Y32}–Cdc42 and AMP_{T32}–Cdc42 does not influence the conformational transitions to the same extent as for AMPylated AMP_{Y77}–Rab1b. The ^{1}H,^{15}N-HSQC-NMR spectra of $AMP_{T35/Y32}$–Cdc42:GTP and $AMP_{T35/Y32}$–Cdc42:GDP are not identical (Fig. 5*A*), indicating that Cdc42-AMPylation does not result in a defined redistribution of the conformational states. Based on a comparison of

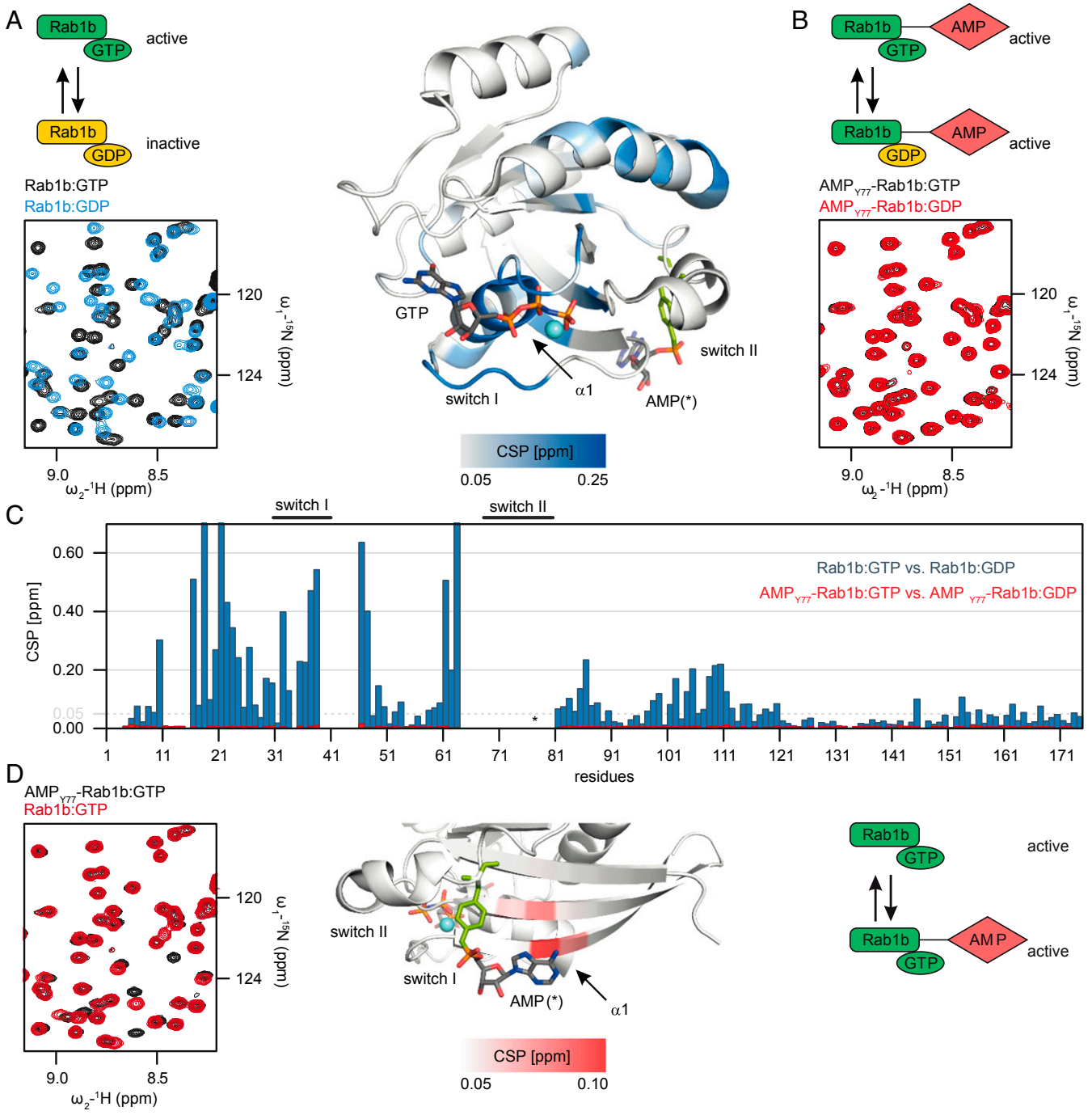

Fig. 3. AMPylation-induced conformational activation of Rab1b:GTP and Rab1b:GDP characterized by NMR spectroscopy. (*A*) Overlay of the ^{1}H,^{15}N-HSQC NMR spectra of the active GTP-bound (black) and the inactive GDP-bound state of Rab1b (blue). Changes in the structural environment are characterized by CSP and plotted onto the crystal structure of AMP$_{Y77}$–Rab1b:GppNHp (PDB code: 3NKV). (*B* and *C*) Effect of AMPylation on the activity state of Rab1b:GTP and Rab1b:GDP. Overlay of the ^{1}H,^{15}N-HSQC NMR spectra of AMP$_{Y77}$–Rab1b:GTP (black) and AMP$_{Y77}$–Rab1b:GDP (red). (*C*) CSP calculated for Rab1b:GTP vs. Rab1b:GDP (blue) and AMPylated AMP$_{Y77}$–Rab1b:GTP vs. AMP$_{Y77}$–Rab1b:GDP (red). (*D*) Overlay of ^{1}H,^{15}N-HSQC NMR spectra of Rab1b:GTP (red) and AMP$_{Y77}$–Rab1b:GTP (black). Changes in the structural environment are characterized by CSP and plotted onto the crystal structure of AMP$_{Y77}$–Rab1b:GppNHp (PDB code: 3NKV; ref. 11). Spectra were recorded at 25 °C in 20 mM Hepes, pH 7.5 in 50 mM NaCl, 1 mM $MgCl_2$, 2 mM DTE, 10 μM GDP, 100 μM DSS. The total protein concentration was 300 μM.

CSPs, the conformation of AMPylated Cdc42 also differ between the nonmodified active (GTP) and inactive (GDP) states in comparison to AMP$_{T35/Y32}$–Cdc42:GTP (Fig. 5*B*). AMPylation of Cdc42:GTP results in a conformational change in the switch II region and helix α1 close to the nucleotide binding site consistent with the CSPs plotted on to the crystal structure of Cdc42:GppNHp (PDB code: 1NF3) (Fig. 5*B*). In contrast, the CSPs deviate much less in the GDP states than in the GTP states, since AMP$_{T35/Y32}$–Cdc42:GDP shows only small CSP differences in comparison to Cdc42:GDP (Fig. 5 *C* and *D*). The conformation of AMP$_{T35/Y32}$–Cdc42:GTP presumably reflects a dynamic average of active and inactive conformational states as suggested by very similar CSPs for

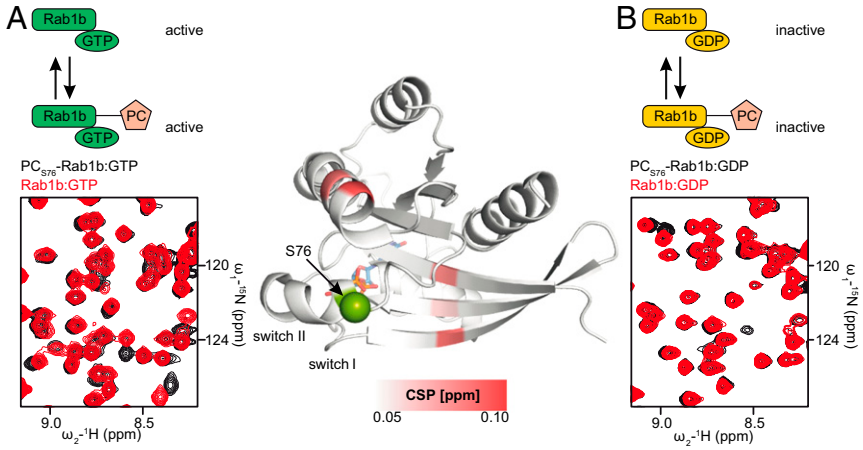

Fig. 4. Phosphocholination-induced effects on Rab1b:GTP and Rab1b:GDP characterized by NMR spectroscopy. (*A*) Overlay of the ^{1}H,^{15}N-HSQC NMR spectra of Rab1b: GTP (red) and PC_{S76}–Rab1b:GTP (black). Changes in the structural environment are characterized by CSP and plotted onto the crystal structure of AMP_{Y77}–Rab1b:GppNHp (PDB code: 3NKV; ref. 11). Residue S76 bearing the PC moiety is indicated as a green sphere. (*B*) Overlay of the ^{1}H,^{15}N-HSQC NMR spectra of the Rab1b:GDP (red) and PC_{S76}–Rab1b:GDP (black). Spectra were recorded at 25 °C in 20 mM Hepes, pH 7.5 in 50 mM NaCl, 1 mM $MgCl_2$, 2 mM DTE, 10 μM GDP, 100 μM DSS. The total protein concentration was 300 μM.

the transition from Cdc42:GTP to $AMP_{T35/Y32}$–Cdc42:GTP (Fig. 5*D*) and the subsequent transition to $AMP_{T35/Y32}$–Cdc42:GDP (*SI Appendix*, Fig. S8*B*).

In conclusion, the observed prolonged duration of the active state of AMP-modified Cdc42:GTP (Fig. 2*B*) can therefore be explained by the NMR data: AMPylation of Cdc42 may switch the GTPase to an intermediate conformational state in $AMP_{T35/Y32}$–Cdc42:GTP that is less competent in hydrolyzing GTP. After GTP hydrolysis, $AMP_{T35/Y32}$–Cdc42:GDP switches back to a conformational state reminiscent of, but not equal to, inactive Cdc42:GDP. Thus, in contrast to Tyr77-AMPylation of Rab1b, the AMPylation of Cdc42 at Tyr32 or Thr35 conformationally affects both nucleotide states.

Discussion

It is challenging to predict the biochemical, functional, and structural consequences of posttranslational modifications reliably. The consequences typically depend on the protein, the type of modification, and the specific position in the protein. The site-specific and preparative introduction of the modification into a particular protein is technically demanding, rendering biochemical and structural studies difficult.

Here, we have established an enzymatic approach to preparatively introduce AMP modifications into Rab1b and Cdc42 and a PC group into Rab1b in a site-specific manner. We have also produced these GTPases in their active and inactive forms in order to study the functional, biochemical, and structural consequences on the different activation states. Using NMR spectroscopy, we were able to monitor very distinct site- and modification-dependent conformational consequences of AMPylation and phosphocholination.

AMPylation of Rab1b at Tyr77 by the *Legionella* enzyme DrrA drastically influences the GTPases' folding stability and distribution of conformational states: First, the presence of the AMP group increases the stability toward thermal unfolding by ∼20 °C in both activation states, but does not impair the general nucleotide binding properties. Second, NMR experiments demonstrate that AMPylation stabilizes the active conformation in the GTP state and additionally forces the proteins into the active conformation in the GDP state. Thus, a PTM of small GTPases has been demonstrated to influence the conformations directly. The AMP modification dominates GDP and GTP binding and permanently forces Rab1b into the active conformation. Interestingly, this active-state promoting effect of Tyr77-AMPylation has been predicted by molecular dynamics simulations recently (19). The negative phosphodiester of the modified amino acid is charged complementarily to a positive surface patch on the GTPase, thereby providing a molecular basis for the switch II stabilization in the active conformation. It is therefore tempting to speculate that other modifications introducing negative charges at Tyr77 may also have a similar impact on the conformations of Rab1b. Recent proteomics analyses on protein phosphorylation have detected a specific modification of Rab1b at Tyr77 (see PhosphoSitePlus for a spectrum of phosphorylation on Rab1b; ref. 29). Consequently, Tyr77 phosphorylation of Rab1b and on homologous positions of related proteins may conformationally activate these GTPases in a similar manner and therefore introduce another level of Rab-activity control that is uncoupling the active state from GDP/GTP loading. It will therefore be interesting to see whether other GTPases may be regulated in a similar manner with phosphorylation inside or outside the switch regions. Recently, phosphorylations of Rab1b at Ser111 and Rab8a/Rab10 at Thr72/Thr73 by PINK1 or LRRK2 have been reported, respectively (30, 31). Since these phosphorylated residues are within or close to the switch II region, similar effects on conformation and dynamics may be induced as seen for Tyr77-AMPylation in the case of Rab1b. Permanent conformational activation of Rab1b by AMPylation may have a functional relevance in the course of *Legionella* infections. The pathogen is recruiting and activating Rab1b at the *Legionella* containing vacuole and likely is dependent on prolonged activation of the Rab protein. Tyr77-AMPylation may thus suit this purpose by inhibiting interaction with GAPs but also by keeping the protein in the active conformation even if Rab1b returns to the GDP form via spontaneous GTP hydrolysis (11, 32). This is also in line with previous reports demonstrating that AMPylation is necessary for Rab1 localization to the LCV (32).

Interestingly, the conformational activation of Rab1b by Tyr77 AMPylation may point at another level of small GTPase regulation that is independent of the GDP and GTP states. In addition, it is tempting to speculate that AMPylation may also modulate cellular protein–protein interaction networks in general by blocking access to specific GTPase sites (e.g., switch II) but still permitting access to other sites (e.g., switch I). It has for example been reported recently that small GTPases can interact with 2 GTP-state specific effectors simultaneously by

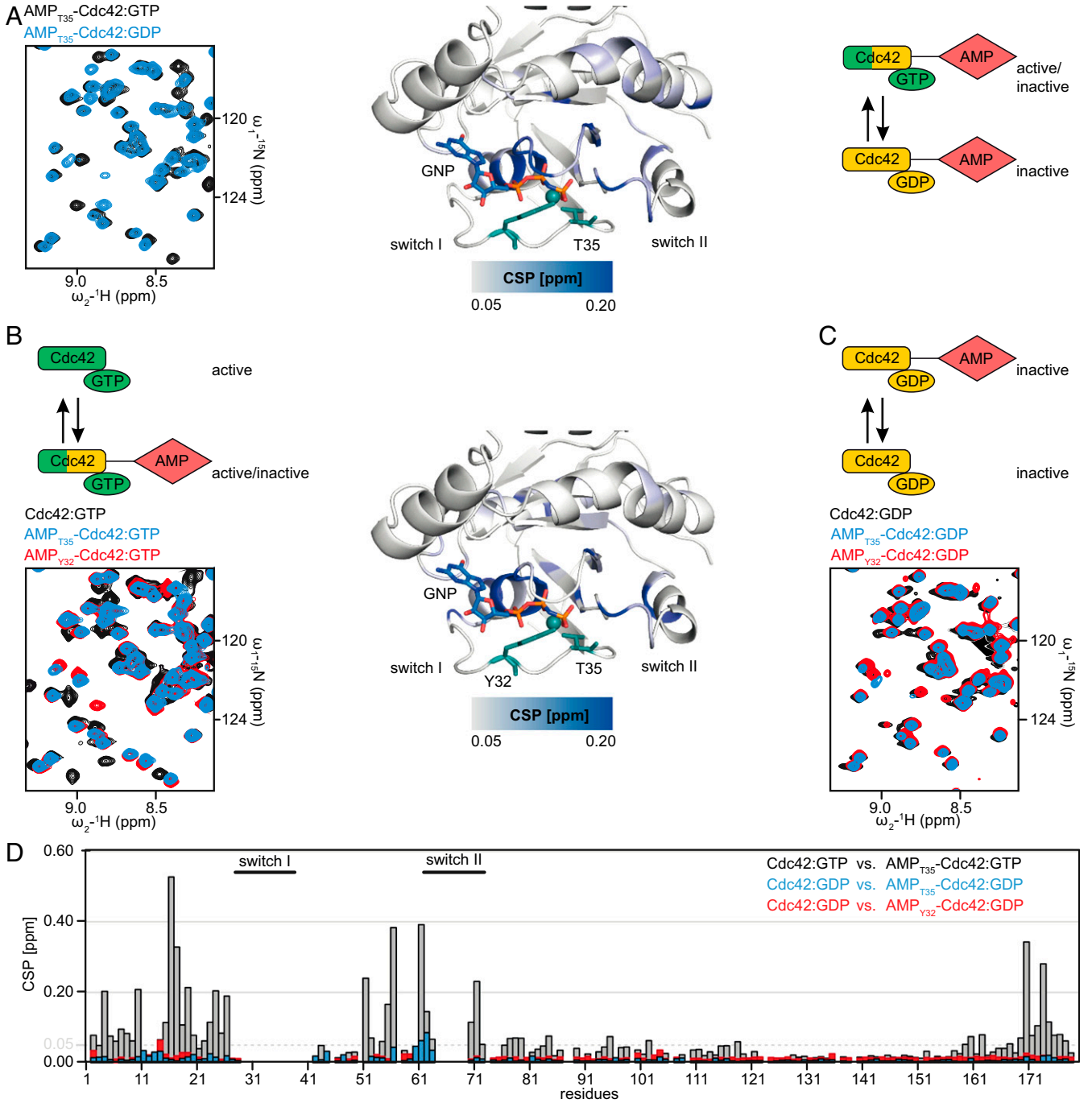

Fig. 5. AMPylation-induced effects on Cdc42:GTP characterized by NMR spectroscopy. (*A*) Conformational effects of AMPylation on AMP$_{T35}$–Cdc42 in different activity states. Overlay of the ^{1}H,^{15}N-HSQC NMR spectra of AMP$_{T35}$–Cdc42 in the GTP (black) and GDP (blue) states. Changes in the vicinity of the covalent modification are characterized by CSP for residues Thr35 and plotted onto the crystal structure of Cdc42:GppNHp (PDB code: 1NF3). (*B*) Cdc42–AMPylation at Tyr32 or Thr35 affects the active state. Overlay of the ^{1}H,^{15}N-HSQC NMR spectra Cdc42:GTP (black), AMP$_{T35}$–Cdc42:GTP (blue), and AMP$_{Y32}$–Cdc42:GTP (red). Changes in the structural environment are characterized by CSP for the modification at Thr35 and plotted onto the crystal structure of Cdc42:GppNHp (PDB code: 1NF3). (*C*) Cdc42–AMPylation at Tyr32 or Thr35 affects the inactive state. Overlay of the ^{1}H,^{15}N-HSQC NMR spectra of Cdc42:GDP (black), AMP$_{T35}$–Cdc42:GDP (blue), and AMP$_{Y32}$–Cdc42:GDP (red). (*D*) CSPs calculated for Cdc42:GTP vs. AMP$_{T35}$–Cdc42:GTP (gray), Cdc42:GDP vs. AMP$_{Y32}$–Cdc42:GDP (red), and Cdc42:GDP vs. AMP$_{T35}$–Cdc42:GDP (blue).

exploiting separate interaction sites: Rab11 interacts with Rabin8 or PI4KIIIβ via switch I exclusively, whereas a different switch I–switch II patch binds to FIP3 (33, 34). It is thus conceivable that modifications such as Tyr77 AMPylation of Rab1b could cause a block of the switch I–switch II binding patch while keeping the GTPase in the active state and thereby permitting binding with GTP-state specific effectors via the switch I patch, even though such an effect has not been observed, yet. Instead, AMPylation appears to affect the binding GTPase effectors exclusively negatively. For example, Cdc42 AMPylation at Thr35 disrupts the interaction with the effector protein PAK (21). IbpA-mediated AMPylation of the Cdc42 relatives RhoA and Rac at Tyr34 and

Tyr32, respectively, block binding to the effector rhotekin (20). Furthermore, Rab1 AMPylation not only impaired binding to the effector protein MICAL-3, but also obstructed interaction with the human GAP TBC1D20, the *Legionella* GAP LepB, and the GDP-state specific protein GDI (11, 35). It is unclear whether AMPylation at Tyr77 is going to affect binding to the numerous reported Rab1 effectors (summarized in ref. 36) similarly as for MICAL-3 or whether some of these may bind to AMPylated Rab1 in both activation states. However, the available complex structures suggest that effectors require binding to the switch II region so that AMPylation likely interferes with complex formation. Nevertheless, it will be interesting to see if a large-scale comparison of effector binding to AMPylated Rab1 and related GTPases may reveal unconventional interaction modes. At least one protein was demonstrated to retain the ability for Rab1–AMP binding: The *Legionella* protein LidA is secreted during infection and can bind to AMPylated and non-AMPylated Rab1 in the GDP and GTP states (10); even so this may be due to an exceptional affinity for the GTPase that may overcome the steric hindrance by the AMP group. Nevertheless, it demonstrates that, in principle, AMPylation is compatible with binding to Rab-specific interactors.

In contrast to Rab1b, enzymatic AMPylation of Cdc42 by VopS at Thr35 or by IbpA at Tyr32 has an intermediate effect on the conformational distribution between the active and inactive states. Neither AMP_{Y32}–Cdc42:GTP or AMP_{T35}–Cdc42:GTP resemble the active (Cdc42:GTP) or the inactive (Cdc42:GDP) states. In contrast, AMP_{Y32}–Cdc42:GDP and AMP_{T35}–Cdc42:GDP show conformational resemblance to the inactive (Cdc42:GDP) state as indicated by ^{1}H,^{15}N-HSQC and ^{31}P NMR experiments. Therefore, a direct activating or inactivating effect of Cdc42 AMPylation cannot be concluded. Rather, the AMP group appears to function as large steric inhibitor of protein–protein interactions and thereby exert their physiological function during infections by blocking Cdc42-dependent protein recruitment (20–22). However, the AMP group unambiguously influences the structure of Cdc42 and therefore impairs interactions with binding partners. It is interesting to note that the steric demand of the AMP group is likely not the only factor contributing to structural changes in Cdc42. Introducing a tryptophan substitution at the Tyr32 site apparently does not change the Cdc42 structure despite of the large increase in bulkiness as claimed previously (37). Consequently, the negative charge of the phosphodiester is likely to contribute to the observed conformational changes, too.

Here, we have shown that AMPylation and phosphocholination of Rab1b or Cdc42 affect the biochemistry and structures of these GTPases very differently. For example, Tyr77-AMPylation forces Rab1b into the active state even if GDP is bound (see Fig. 6 for a schematic summary of the results). In contrast, Ser76 phosphocholination does not interfere with the normal activity states of Rab1b: Conformationally, PC_{S76}–Rab1b:GTP and Rab1b:GTP are equivalent, as are PC_{S76}–Rab1b:GDP and Rab1b:GDP. In the case of Cdc42 AMPylation, the situation is more complicated in comparison to Rab1b AMPylation. Modification at Tyr32 or Thr35 results in two further conformational states that are not identical to the active GTP or the inactive GDP states. It would be interesting to investigate whether these conformational switching activities of PTMs are only relevant in the context of infections with bacterial pathogens or whether eukaryotes exploit such conformational control mechanism during homeostasis as a regular GTPase control mechanism.

Methods

Protein Expression and Purification. $DrrA_{340–533}$, $DrrA_{8–533}$, $SidD_{1–507}$, $TBC1D20_{1–362}$, $AnkX_{1–800}$, $Lem3_{1–570}$, and $Rab1b_{3–174}$ were purified as described previously (8, 11, 16, 38).

In brief, genes encoding for DrrA, SidD, TBC1D20, AnkX, and Lem3 were cloned in a pET19 vector with N-terminal hexa-histidine-tag (His_6-tag) and a tobacco etch virus (TEV) cleavage site. Genes encoding for $IbpA_{3483–3797}$, $VopS_{31–387}$, and $Dock9_{1605–2032}$ were cloned in a pMAL vector including a His_6-maltose-binding-protein (MBP)-tag and a TEV cleavage site. Protein production in *Escherichia coli* BL21 Codon Plus (DE3) RIL cells was induced by addition of 0.5 mM isopropyl β-D-1-thiogalactopyranoside (IPTG) over night at 20 °C. Purification was achieved by nickel affinity chromatography, TEV cleavage of the His_6-tag or His-MBP-tag, and final gel filtration in 20 mM Hepes pH 7.5; 100 mM NaCl; 2 mM dithioerythritol (DTE); 1 mM $MgCl_2$. For $Lem3_{1–570}$ 5% glycerol was added to all buffers.

$Rab1b_{3–174}$ Q67A and $Cdc42_{1–188}$ Q61L were produced as fusions with the maltose binding protein in *E. coli* BL21 (DE3) cells using the pMAL (Rab1b) or pOPINM (Cdc42) vector. Genes encoding for $Cdc42_{1–179}$ Q61A/L were cloned in a pGEX4T1 vector and purified as fusions with a glutathione S-transferase tag. Rab1b and Cdc42 mutant proteins were generated by site-directed mutagenesis.

Isotopically labeled proteins were produced by overexpression in *E. coli* BL21 (DE3) cells in M9 minimal medium supplemented with ^{15}N, ^{13}C, and/or ^{2}H. Production of ^{15}N and $^{13}C^{15}N$ labeled proteins was performed using $^{15}NH_4Cl$ (1 g/L) and ^{13}C-D-glucose (2 g/L) as sole nitrogen and carbon sources. For partial random deuteration, H_2O in M9 medium was substituted subsequently with increasing concentrations of D_2O. After adaptation of *E. coli* cells, protein expression was carried out in 90% D_2O M9 medium.

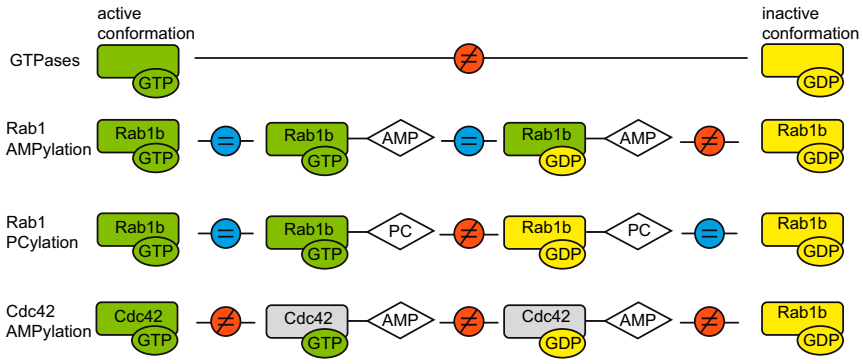

Fig. 6. PTMs affect GTPase conformations differently (conformationally identical or nonidentical states are indicated by an equal sign or unequal sign, respectively). Classically, GTPases such as Rab1b differ strongly in their active, GTP-bound and inactive, GDP-bound conformations. Tyr77–AMPylation of Rab1b results in a redistribution of conformational states in favor of the active form. That is, AMP_{Y77}–Rab1b:GDP is conformationally identical to active Rab1b:GTP but not inactive Rab1b:GDP. Ser76 phosphocholination of Rab1b, instead, retains the normal distribution of conformational states (i.e., GDP bound is inactive, GTP state is active). In contrast, Tyr32 and Thr35 AMPylation of Cdc42:GDP and Cdc42:GTP results in the formation of two additional conformational states. Here, the AMP-modified states do not resemble either the active or the inactive states (green, yellow, gray: active, inactive, and intermediate states, respectively; blue and red: equal and nonidentical conformations, respectively).

Unlabeled and isotopically labeled Rab proteins were produced at 25 °C overnight after induction with 0.5 mM IPTG at OD 0.6 to 0.8. Proteins were purified by nickel affinity chromatography, followed by TEV cleavage of the His_6–MBP tag and final gel filtration in 20 mM Hepes pH 8.0; 50 mM NaCl; 2 mM DTE; 1 mM $MgCl_2$; 10 μM GDP. For protein yields see *SI Appendix*, Table S1.

Preparative Nucleotide Exchange. Nucleotide exchange of Rab1b proteins was performed as described earlier (11). Rab proteins were incubated with 5 mM ethylenediaminetetraacetic acid (EDTA) and a 20 times molar excess of nucleotide at 25 °C for at least 2 h in exchange buffer (20 mM Hepes pH 8.0; 50 mM NaCl, 2 mM DTE). Excess nucleotide was removed by using a PD-10 column (GE Healthcare) equilibrated in 20 mM Hepes pH 8.0; 50 mM NaCl; 2 mM DTE; 1 mM $MgCl_2$; 10 μM nucleotide). Completeness of the exchange was verified by reversed-phase high-performance liquid chromatography (HPLC) analysis.

Preparative AMPylation/Phosphocholination. Preparative modification of Rab1b was performed as described earlier (11). The protein was incubated with a 2.5 molar excess of nucleotide (ATP; CDP-choline) and a 0.01 molar ratio of the respective enzyme (DrrA; AnkX) at room temperature until 100% modification was achieved. Completeness of the reaction was verified by mass spectrometry. The modified protein was purified by size exclusion chromatography (20 mM Hepes pH 8.0; 50 mM NaCl, 2 mM DTE; 1 mM $MgCl_2$; 10 μM GDP).

Reversed-Phase HPLC Analysis. Analysis of the nucleotide state of Rab proteins was performed by reversed-phase HPLC analysis on a C18 Prontosil column (Bischoff). A sample (1 nmol) of the GTPase was denatured at 95 °C for 5 min to release bound nucleotide, protein was separated by centrifugation, and nucleotide supernatant applied to the C18 column. Separation of nucleotides was conducted in 50 mM potassium phosphate pH 6.6, 10 mM tetrabutyl-ammonium-bromide, and 12% acetonitrile at 1 mL/min for 20 min.

Electrospray Ionization Mass Spectrometry (ESI-MS). To test for successful modification of protein, ESI-MS was used. The respective protein solution (50 μM) was desalted by using C4-zip-tips (Millipore). C4 material was equilibrated with 10 μl of 50% acetonitrile and 2 times 10 μl of 0.1% formic acid, then 10 μl of protein solution was loaded. The bound proteins were washed 2 times with 0.1% formic acid and eluted with 50% acetonitrile; 5 μl of the protein solution was applied to the LCQ fleet mass spectrometer (Thermo Scientific). Ion spectra were generated with Xcalibur (Thermo Scientific) and deconvoluted using MagTran (39).

Determination of Intrinsic Nucleotide Exchange Rates. Intrinsic nucleotide exchange rates of small GTPases were determined by measuring release of mant-nucleotides in a fluorescence spectrophotometer (Fluoromax 4; Horiba Scientific) with excitation at 360 nm and emission at 440 nm at 25 °C in 20 mM Hepes, pH 7,5; 50 mM NaCl; 5 mM $MgCl_2$, and 2 mM DTE. Release of mant-nucleotide was triggered by addition of 100 × GDP or GTP. Excitation and emission slits were set to 1 and 5 nm, respectively.

Determination of Intrinsic Hydrolysis Rates. Preparatively GTP loaded GTPases were incubated at 25 °C in 20 mM Hepes, 50 mM NaCl, 1 mM $MgCl_2$, 2 mM DTE. Samples were taken at indicated time points and subjected to reversed-phase HPLC analysis.

Circular Dichroism Spectroscopy. Thermal stability of unmodified/modified GTPases was investigated by CD Spectroscopy. Measurements of CD spectra were carried out in a JASCO 715 CD Spectrometer equipped with a Peltier-temperature controller. Spectra were measured at 15 μM protein concentration in a quartz cuvette with 1 mm path length (Hellma) in 2 mM Hepes pH 7.5; 20 mM NaCl; 1 mM $MgCl_2$; 10 μM GDP. Temperature was increased by 20 °C/h and molar ellipticity was measured at 222 nm.

NMR Spectroscopy. All NMR spectra were recorded at 25 °C in 20 mM Hepes, pH 7.5 in 50 mM NaCl, 1 mM $MgCl_2$, 2 mM DTE, 10 μM GDP or GTP, 100 μM sodium trimethylsilylpropanesulfonate (DSS). The total protein concentration was 300 μM; ^1H,^{15}N-HSQC NMR correlation spectra were recorded on a Bruker Avance III 600 MHz spectrometer equipped with a 5 mm TCI CryoProbe with a Z-gradient using 2048 × 256 data points in t_2 and t_1 and 4 scans, respectively.

The backbone resonances of the unmodified Rab1b (bound to GTP or GDP) were assigned using conventional 3D-HNCACB, HNCO, HNCA, HN(CA)CO, and HN(CO)CA experiments, recorded on Bruker AV III 600, 800, or 900 MHz NMR spectrometers equipped with 5 mm TCI CryoProbes with Z-gradients. The amide resonances of the unmodified Cdc42 (bound to GTP or GDP) were assigned based on the BMRB database (code: 15424) and further confirmed using 3D ^1H,^{15}N-NOESY-HSQC spectra recorded at 600 or 900 MHz proton Larmor frequency using a mixing time of 120 ms. All amide resonances of the modified (AMPylation or phosphocholination) Rab1b and Cdc42 were assigned based on the assignments of the unmodified proteins and confirmed by 3D ^1H,^{15}N-NOESY-HSQC spectra, as described above.

Changes in ^1H and ^{15}N chemical shifts (parts per million) were calculated as $\Delta\delta_{CSP} = \left[\Delta\delta_{HN}^2 + \left(\frac{\Delta\delta_N}{R_{scale}}\right)^2\right]^{1/2}$, where the chemical shift scaling factor, R_{scale}, is given by the ratio of the average variances, $\langle\sigma_\delta\rangle_{HN}/\langle\sigma_\delta\rangle_N$, of amide proton and nitrogen chemical shifts as described (40). Chemical shift perturbations were plotted onto the crystal structure of AMP_{Y77}–Rab1b:GppNHp (PDB code: 3NKV) and Cdc42:GppNHp (PDB code: 1NF3) using the program PyMol.

^{15}N T_1 relaxation times were obtained using relaxation delays of 750; 500; 10; 500; 1,000; 300; 1,250; 1,800; 100; and 1,250 ms. For measurement of ^{15}N T_2 relaxation times, delays of 0; 130; 16,3; 65,3; 114,2; 49,0; 65,3; 16,3; 81,6; and 97,9 ms were used. The spectra were recorded at 298 K using 1,800 × 256 data points, a spectral widths of 18 × 35 ppm in t_2 and t_1, respectively, and eight scans per t_1 increment on Bruker AV III 600 MHz spectrometer equipped with a 5 mm TCI Cryoprobe with a Z-gradient. {^1H}-^{15}N heteronuclear nuclear Overhauser effect values were measured interleaved, using 1,800 × (2 × 230) data points, spectral widths of 18 × 35 ppm, and 100 scans per t_1 increment.

Data Availability Statement. NMR chemical shift assignments are deposited in the BMRB database; Rab1b:GTP (BMRB 50172) (41), Rab1b:GDP (BMRB 50173) (42), AMPY77–Rab1b:GTP (BMRB 50174) (43), AMPY77–Rab1b:GDP (BMRB 50175) (44), PCS76–Rab1b:GTP (BMRB 50176) (45), PCS76–Rab1b:GDP (BMRB 50177) (46), Cdc42:GTP (BMRB 50178) (47), Cdc42:GDP (BMRB 50179) (48), AMPT35–Cdc42:GTP (BMRB 50180) (49), AMPT35–Cdc42:GDP (BMRB 50181) (50), AMPY32–Cdc42:GTP (BMRB 50182) (51), AMPY32–Cdc42:GDP (BMRB 50183) (52).

ACKNOWLEDGMENTS. This work was supported by the SFB1035 (German Research Foundation (Deutsche Forschungsgemeinschaft, DFG), Sonderforschungsbereich SFB1035, projects B03 and B05) and by the Helmholtz Association Initiative and Networking Fund (project ZT-I-0003 to M.S.). Matthias Müller is acknowledged for critically commenting on the manuscript. We acknowledge access to NMR spectrometers at the Bavarian NMR Center (BNMRZ, Garching). A.I. acknowledges access to the core facilities and laboratories of the Centre for Structural Systems Biology (CSSB, Hamburg).

1. T. W. Traut, Physiological concentrations of purines and pyrimidines. *Mol. Cell. Biochem.* **140**, 1–22 (1994).
2. J. Cherfils, M. Zeghouf, Regulation of small GTPases by GEFs, GAPs, and GDIs. *Physiol. Rev.* **93**, 269–309 (2013).
3. J. Huang *et al.*, Antibacterial autophagy occurs at PI(3)P-enriched domains of the endoplasmic reticulum and requires Rab1 GTPase. *Autophagy* **7**, 17–26 (2011).
4. F. C. M. Zoppino, R. D. Militello, I. Slavin, C. Alvarez, M. I. Colombo, Autophagosome formation depends on the small GTPase Rab1 and functional ER exit sites. *Traffic* **11**, 1246–1261 (2010).
5. N. Dong *et al.*, Structurally distinct bacterial TBC-like GAPs link Arf GTPase to Rab1 inactivation to counteract host defenses. *Cell* **150**, 1029–1041 (2012).
6. T. Murata *et al.*, The *Legionella pneumophila* effector protein DrrA is a Rab1 guanine nucleotide-exchange factor. *Nat. Cell Biol.* **8**, 971–977 (2006).
7. M. P. Machner, R. R. Isberg, Targeting of host Rab GTPase function by the intravacuolar pathogen *Legionella pneumophila*. *Dev. Cell* **11**, 47–56 (2006).
8. S. Schoebel, L. K. Oesterlin, W. Blankenfeldt, R. S. Goody, A. Itzen, RabGDI displacement by DrrA from *Legionella* is a consequence of its guanine nucleotide exchange activity. *Mol. Cell* **36**, 1060–1072 (2009).
9. A. Ingmundson, A. Delprato, D. G. Lambright, C. R. Roy, *Legionella pneumophila* proteins that regulate Rab1 membrane cycling. *Nature* **450**, 365–369 (2007).
10. S. Schoebel, A. L. Cichy, R. S. Goody, A. Itzen, Protein LidA from Legionella is a Rab GTPase supereffector. *Proc. Natl. Acad. Sci. U.S.A.* **108**, 17945–17950 (2011).
11. M. P. Müller *et al.*, The *Legionella* effector protein DrrA AMPylates the membrane traffic regulator Rab1b. *Science* **329**, 946–949 (2010).
12. M. P. Müller *et al.*, Characterization of enzymes from *Legionella pneumophila* involved in reversible adenylylation of Rab1 protein. *J. Biol. Chem.* **287**, 35036–35046 (2012).
13. M. R. Neunuebel *et al.*, De-AMPylation of the small GTPase Rab1 by the pathogen *Legionella pneumophila*. *Science* **333**, 453–456 (2011).
14. Y. Tan, Z. Q. Luo, *Legionella pneumophila* SidD is a deAMPylase that modifies Rab1. *Nature* **475**, 506–509 (2011).

15. S. Mukherjee *et al*., Modulation of Rab GTPase function by a protein phosphocholine transferase. *Nature* **477**, 103–106 (2011).
16. P. R. Goody *et al*., Reversible phosphocholination of Rab proteins by *Legionella pneumophila* effector proteins. *EMBO J.* **31**, 1774–1784 (2012).
17. Y. Tan, R. J. Arnold, Z. Q. Luo, *Legionella pneumophila* regulates the small GTPase Rab1 activity by reversible phosphorylcholination. *Proc. Natl. Acad. Sci. U.S.A.* **108**, 21212–21217 (2011).
18. E. H. Sklan *et al*., TBC1D20 is a Rab1 GTPase-activating protein that mediates hepatitis C virus replication. *J. Biol. Chem.* **282**, 36354–36361 (2007).
19. M. P. Luitz, R. Bomblies, E. Ramcke, A. Itzen, M. Zacharias, Adenylylation of Tyr77 stabilizes Rab1b GTPase in an active state: A molecular dynamics simulation analysis. *Sci. Rep.* **6**, 19896 (2016).
20. C. A. Worby *et al*., The fic domain: Regulation of cell signaling by adenylylation. *Mol. Cell* **34**, 93–103 (2009).
21. M. L. Yarbrough *et al*., AMPylation of Rho GTPases by *Vibrio* VopS disrupts effector binding and downstream signaling. *Science* **323**, 269–272 (2009).
22. S. Mattoo *et al*., Comparative analysis of *Histophilus somni* immunoglobulin-binding protein A (IbpA) with other fic domain-containing enzymes reveals differences in substrate and nucleotide specificities. *J. Biol. Chem.* **286**, 32834–32842 (2011).
23. J. John *et al*., Kinetic and structural analysis of the Mg(2+)-binding site of the guanine nucleotide-binding protein p21H-ras. *J. Biol. Chem.* **268**, 923–929 (1993).
24. E. F. Pai *et al*., Refined crystal structure of the triphosphate conformation of H-ras p21 at 1.35 A resolution: Implications for the mechanism of GTP hydrolysis. *EMBO J.* **9**, 2351–2359 (1990).
25. N. Abdul-Manan *et al*., Structure of Cdc42 in complex with the GTPase-binding domain of the 'Wiskott-Aldrich syndrome' protein. *Nature* **399**, 379–383 (1999).
26. C. J. Der, T. Finkel, G. M. Cooper, Biological and biochemical properties of human rasH genes mutated at codon 61. *Cell* **44**, 167–176 (1986).
27. M. Geyer, C. Wilde, J. Selzer, K. Aktories, H. R. Kalbitzer, Glucosylation of Ras by *Clostridium sordellii* lethal toxin: Consequences for effector loop conformations observed by NMR spectroscopy. *Biochemistry* **42**, 11951–11959 (2003).
28. S. M. Garrard *et al*., Structure of Cdc42 in a complex with the GTPase-binding domain of the cell polarity protein, Par6. *EMBO J.* **22**, 1125–1133 (2003).
29. P. V. Hornbeck *et al*., PhosphoSitePlus, 2014: Mutations, PTMs and recalibrations. *Nucleic Acids Res.* **43**, D512–D520 (2015).
30. Y. C. Lai *et al*., Phosphoproteomic screening identifies Rab GTPases as novel downstream targets of PINK1. *EMBO J.* **34**, 2840–2861 (2015).
31. M. Steger *et al*., Phosphoproteomics reveals that Parkinson's disease kinase LRRK2 regulates a subset of Rab GTPases. *eLife* **5**, e12813 (2016).
32. C. A. Hardiman, C. R. Roy, AMPylation is critical for Rab1 localization to vacuoles containing Legionella pneumophila. *mBio* **5**, e01035-13 (2014).
33. J. E. Burke *et al*., Structures of PI4KIIIβ complexes show simultaneous recruitment of Rab11 and its effectors. *Science* **344**, 1035–1038 (2014).
34. M. Vetter, R. Stehle, C. Basquin, E. Lorentzen, Structure of Rab11-FIP3-Rabin8 reveals simultaneous binding of FIP3 and Rabin8 effectors to Rab11. *Nat. Struct. Mol. Biol.* **22**, 695–702 (2015).
35. L. K. Oesterlin, R. S. Goody, A. Itzen, Posttranslational modifications of Rab proteins cause effective displacement of GDP dissociation inhibitor. *Proc. Natl. Acad. Sci. U.S.A.* **109**, 5621–5626 (2012).
36. A. H. Hutagalung, P. J. Novick, Role of Rab GTPases in membrane traffic and cell physiology. *Physiol. Rev.* **91**, 119–149 (2011).
37. H. Rensland *et al*., Substrate and product structural requirements for binding of nucleotides to H-ras p21: The mechanism of discrimination between guanosine and adenosine nucleotides. *Biochemistry* **34**, 593–599 (1995).
38. K. Heller *et al*., Covalent protein labeling by enzymatic phosphocholination. *Angew. Chem. Int. Ed. Engl.* **54**, 10327–10330 (2015).
39. Z. Zhang, A. G. Marshall, A universal algorithm for fast and automated charge state deconvolution of electrospray mass-to-charge ratio spectra. *J. Am. Soc. Mass Spectrom.* **9**, 225–233 (1998).
40. F. A. A. Mulder, D. Schipper, R. Bott, R. Boelens, Altered flexibility in the substrate-binding site of related native and engineered high-alkaline Bacillus subtilisins. *J. Mol. Biol.* **292**, 111–123 (1999).
41. H.-S. Kang, K. Barthelmes, M. Sattler, Rab1b bound to GTP. Biological Magnetic Resonance Data Bank. http://www.bmrb.wisc.edu/data_library/summary/index.php?bmrbId=50172. Deposited 28 January 2020.
42. H.-S. Kang, K. Barthelmes, M. Sattler, Rab1b bound to GDP. Biological Magnetic Resonance Data Bank. http://www.bmrb.wisc.edu/data_library/summary/index.php?bmrbId=50173. Deposited 28 January 2020.
43. H.-S. Kang, K. Barthelmes, M. Sattler, Rab1b bound to GTP (AMPylation at Tyr77). Biological Magnetic Resonance Data Bank. http://www.bmrb.wisc.edu/data_library/summary/index.php?bmrbId=50174. Deposited 28 January 2020.
44. H.-S. Kang, K. Barthelmes, M. Sattler, Rab1b bound to GDP (AMPylation at Tyr77). Biological Magnetic Resonance Data Bank. http://www.bmrb.wisc.edu/data_library/summary/index.php?bmrbId=50175. Deposited 28 January 2020.
45. H.-S. Kang, K. Barthelmes, M. Sattler, Rab1b bound to GTP (Phosphocholination at Ser76). Biological Magnetic Resonance Data Bank. http://www.bmrb.wisc.edu/data_library/summary/index.php?bmrbId=50176. Deposited 28 January 2020.
46. H.-S. Kang, K. Barthelmes, M. Sattler, Rab1b bound to GDP (Phosphocholination at Ser76). Biological Magnetic Resonance Data Bank. http://www.bmrb.wisc.edu/data_library/summary/index.php?bmrbId=50177. Deposited 28 January 2020.
47. H.-S. Kang, K. Barthelmes, M. Sattler, Cdc42 bound to GTP. Biological Magnetic Resonance Data Bank. http://www.bmrb.wisc.edu/data_library/summary/index.php?bmrbId=50178. Deposited 28 January 2020.
48. H.-S. Kang, K. Barthelmes, M. Sattler, Cdc42 bound to GDP. Biological Magnetic Resonance Data Bank. http://www.bmrb.wisc.edu/data_library/summary/index.php?bmrbId=50179. Deposited 28 January 2020.
49. H.-S. Kang, K. Barthelmes, M. Sattler, Cdc42 bound to GTP (AMPylation at Thr35). Biological Magnetic Resonance Data Bank. http://www.bmrb.wisc.edu/data_library/summary/index.php?bmrbId=50180. Deposited 28 January 2020.
50. H.-S. Kang, K. Barthelmes, M. Sattler, Cdc42 bound to GDP (AMPylation at Thr35). Biological Magnetic Resonance Data Bank. http://www.bmrb.wisc.edu/data_library/summary/index.php?bmrbId=50181. Deposited 28 January 2020.
51. H.-S. Kang, K. Barthelmes, M. Sattler, Cdc42 bound to GTP (AMPylation at Tyr32). Biological Magnetic Resonance Data Bank. http://www.bmrb.wisc.edu/data_library/summary/index.php?bmrbId=50182. Deposited 28 January 2020.
52. H.-S. Kang, K. Barthelmes, M. Sattler, Cdc42 bound to GDP (AMPylation at Tyr32). Biological Magnetic Resonance Data Bank. http://www.bmrb.wisc.edu/data_library/summary/index.php?bmrbId=50183. Deposited 28 January 2020.